ACS OMEGA

http://pubs.acs.org/journal/acsodf

Article

Epigallocatechin Gallate Protects Mice against Methionine–Choline-Deficient-Diet-Induced Nonalcoholic Steatohepatitis by Improving Gut Microbiota To Attenuate Hepatic Injury and Regulate Metabolism

Kaiting Ning, Kaikai Lu, Qian Chen, Zizhen Guo, Xiaojuan Du, Farooq Riaz, Lina Feng, Yuping Fu, Chunyan Yin, Fujun Zhang, Litao Wu, and Dongmin Li*

Cite This: *ACS Omega* 2020, 5, 20800–20809

Read Online

ACCESS | Metrics & More | Article Recommendations | Supporting Information

ABSTRACT: Epigallocatechin gallate (EGCG) has been regarded as a protective bioactive polyphenol in green tea against nonalcoholic steatohepatitis (NASH), but the mechanism remains poorly deciphered. Herein, we assessed the role and mechanism of EGCG on gut microbiota and the metabolism in NASH development. Forty-eight male C57BL/6J mice were fed with either a methionine–choline-sufficient diet or a methionine–choline-deficient (MCD) diet with or without EGCG administration for 4 weeks. Liver injury, inflammation, lipid accumulation, and iron overload were examined. 16S ribosomal RNA sequencing was used to detect the fecal microbiome. In our research, we observed that EGCG notably improved MCD-diet-derived gut microbiota dysbiosis, as proved by a distinctively clustered separation from that of the MCD group and by the decrease of the *Oxalobacter*, *Oscillibacter*, *Coprococcus_1*, and *Desulfovibrio* genera and enrichment of *norank_f__Bacteroidales_S24_7_group*, *Alloprevotella*, and *Bacteroides*. Spearman-correlation heatmap analysis indicated that *Bacteroides* and *Alloprevotella* induced by EGCG were strongly negatively correlated with lipid accumulation. Functional enzymes of the gut microbiome were predicted by PICRUSt based on the operation classification unit. The results revealed that 1468 enzymes were involved in various metabolic pathways, and 371 enzymes showed distinct changes between untreated and EGCG-treated mice. Long-chain-fatty-acid-CoA ligase ACSBG played a distinct role in fatty acid metabolism and ferroptosis and was significantly negatively correlated with *Bacteroides*. Altogether, the salutary effect of EGCG on NASH might be via shifting gut flora and certain enzymes from genera. Our study thus takes a step toward NASH prevention and therapy.

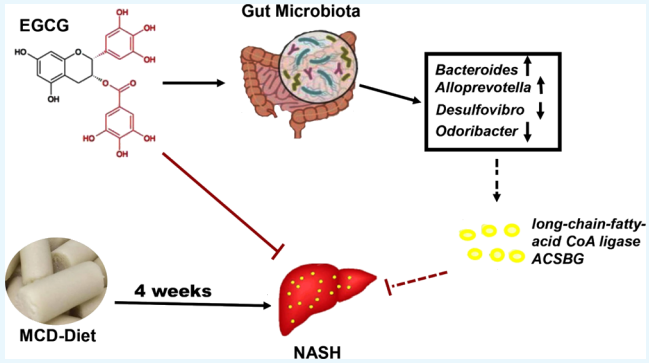

INTRODUCTION

Nonalcoholic fatty liver disease (NAFLD) is a condition of the chronic liver disorder around the globe and associated with metabolic syndromes such as obesity, insulin resistance, and diabetes.[1] The etiology of NAFLD is unclear, though genetic factors, environmental factors, lifestyle, etc., were implicated.[1] Therapeutic treatment options are limited, and no effective drug has been used in clinics to intervene NAFLD now.[2,3]

Mounting evidence suggests that gut dysbiosis is related to chronic liver disorders.[4−7] Gut microbiota, harboring a complex structure and substantial genes, has emerged as a critical environmental factor involved in the process of liver disorders through the gut–liver axis.[8] Lipopolysaccharide (LPS), a main gut bacterial product, can disturb the microbiota homeostasis, impair the intestinal barrier function driving bacterial translocation, and also flow into the liver via the portal vein, triggering chronic hepatic diseases.[9−12] Apart from LPS, short-chain fatty acids (SCFAs) are primarily derived from dietary carbohydrates catalyzed by the gut flora which greatly served to maintain the intestinal barrier, thus preventing NAFLD.[13,14]

Nonalcoholic steatohepatitis (NASH) is a necessary stage of NAFLD for the development of simple steatosis to cirrhosis and hepatocellular carcinoma. Recent studies also highlighted that the accumulation of free cholesterol can exacerbate NASH.[15,16] Furthermore, iron loading also contributed to liver damage.[17] Reactive oxygen species can be produced via iron catalyzing, and increasing iron levels also enhance lipid peroxidation to cause cellular damage.[17−21]

Received: April 13, 2020
Accepted: July 29, 2020
Published: August 12, 2020

https://dx.doi.org/10.1021/acsomega.0c01689
ACS Omega 2020, 5, 20800–20809

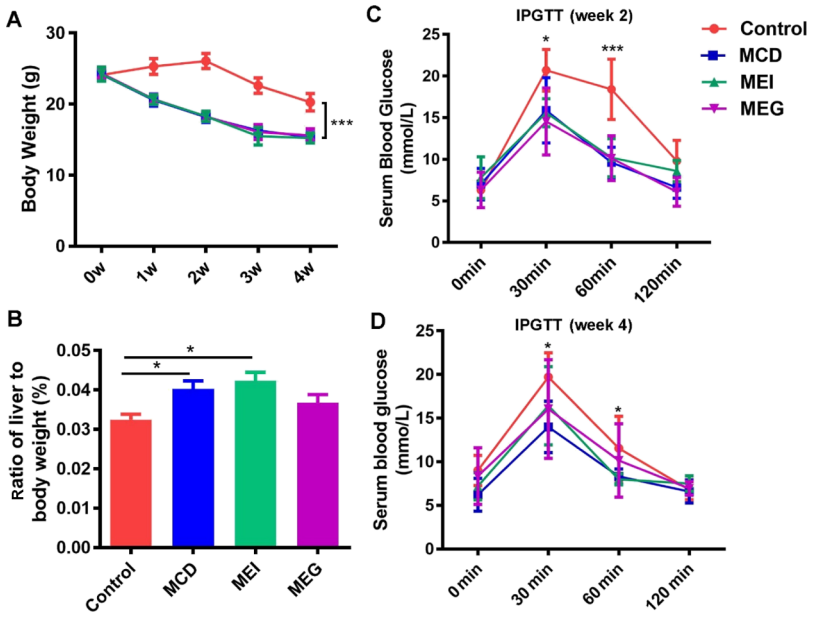

Figure 1. Effects of EGCG on MCD-induced body loss, liver weight/body weight ratio, and IPGTT change. (A) Body weights were measured weekly for C57BL/6J mice on the MCS diet or the MCD diet with or without EGCG (50 mg/kg body weight) supplementation for 4 weeks. Control group: MCS diet for 4 weeks; MCD group: MCD diet for 4 weeks; MEI group: 2 week MCD diet +2 week EGCG i.p. (50 mg/kg); MEG group: 2 week MCD diet + gavage with 50 mg/kg of EGCG for 2 weeks ($n = 7-11$). (B) Four groups of mice were euthanized; then, the liver was collected and weighed, and the liver weight/body weight ratio was calculated ($n = 6-10$). (C,D) Each mouse was injected i.p. with 2 g/kg body weight of glucose and subjected to evaluation of serum blood glucose before (C) and after EGCG supplementation (D) ($n = 6-11$). All the above results were analyzed using GraphPad Prism Version 6. The values were shown as the mean ± SD values of each group (*$P < 0.05$, **$P < 0.01$, ***$P < 0.001$, *$P < 0.05$ vs the control group).

Green tea, a popular beverage in the world,[22] contains health-promoting compounds such as polyphenols. Epigallocatechin gallate (EGCG), one of the tea polyphenols, exerts various salutary effects such as antioxidative, anticarcinogenic, anti-inflammatory, antiviral, antibacterial, antihypertensive, and hypocholesterolemic effects.[23−26] Mounting evidence indicated that the primary green tea catechin EGCG alone was amazingly against body fat accumulation[27−30] and progress of fatty liver in mice fed with a high-fat diet[29−31] or a methionine−choline-deficient (MCD) diet.[32] Additionally, there were many different ways and doses to treated mice with EGCG for NASH therapy, such as 0.1% in water;[33] 3.2 g/kg in the diet;[34] 10, 20, and 40 mg/kg/d i.p.;[35] 50 mg/kg 0.1 mL/day by gavage;[36] and so on. Therefore, we hypothesized EGCG to exert a protective effect on NASH through reshaping gut microbiota to alter the metabolic status.

In our current study, we reported that two primary administration ways of EGCG (gavage and intraperitoneal injection) notably moderated NASH driven by the MCD diet in mice. EGCG shifted the gut microbiota; reduced the liver injury, lipid accumulation, and iron overload; and thus protected against liver steatosis. This study gives us a new insight of EGCG protection against NAFLD.

RESULTS

EGCG Reduced Body Weight Loss and the Ratio of Liver Weight to Body Weight and Regulated Serum Blood Glucose in MCD-Fed Mice. As we expected, MCD-fed mice gained a less weight than control mice ($p < 0.001$). However, EGCG did not successfully prevent MCD mice from losing more weight (Figure 1A), which was accompanied by the significantly decreased ratio of liver weight to body weight only in MEG mice ($p < 0.05$) (Figure 1B). Meanwhile, as shown in Figure 1C, the serum blood glucose level in MCD-fed mice was dramatically lower than that in the control group within 30−60 min after i.p. injection of 2 g/kg glucose (intraperitoneal glucose tolerance test, IPGTT) ($p < 0.05$, $p < 0.001$). After 2 weeks of EGCG treatment, compared with the control group, the serum blood glucose level in MCD-fed mice was significantly decreased within 30−60 min after i.p. injection of glucose (IPGTT) ($p < 0.05$), and the serum blood glucose level of MEI and MEG mice is slightly higher than that of MCD mice but has no significance with MCD mice (Figure 1D). MGI and MEG showed no significant difference.

EGCG Alleviated Hepatic Injury, Lipid Accumulation, Fibrosis Progression, Iron-Ion Loading, and Plasma Parameters in MCD-Fed Mice. We found that the liver sections from the MCD group showed extensive macrovesicular fat accumulation, which is related to inflammatory infiltration (Figure 2A). However, two EGCG intervention groups showed lower microvesicular steatosis and inflammatory foci in the liver (Figure 2A). Oil red O (ORO) staining was used to assess neutral lipid accumulations in liver tissues. Visualization and quantification of neutral lipids by ORO analysis found that there are more lipids loaded in the MCD group, and after treatment with EGCG, MEI and MEG showed reverse effects (Figure 2B). According to Figure 2C, the control group showed a normal lobular structure with veins and radial hepatic cords in the liver. MCD mice displayed character of fibrosis including periportal and interstitial collagen deposition, which showed blue after Masson's trichrome staining. The MEI and MEG groups showed notable improvements in liver fibrosis, as proven by a surprising decrease in the collagen-stained area in the liver sections. Next, we evaluated iron accumulation by Prussian blue staining. The MCD group showed obvious iron accumulation compared to the control group ($p < 0.001$), and two EGCG administration groups (the MEI and MEG groups) showed

https://dx.doi.org/10.1021/acsomega.0c01689
ACS Omega 2020, 5, 20800−20809

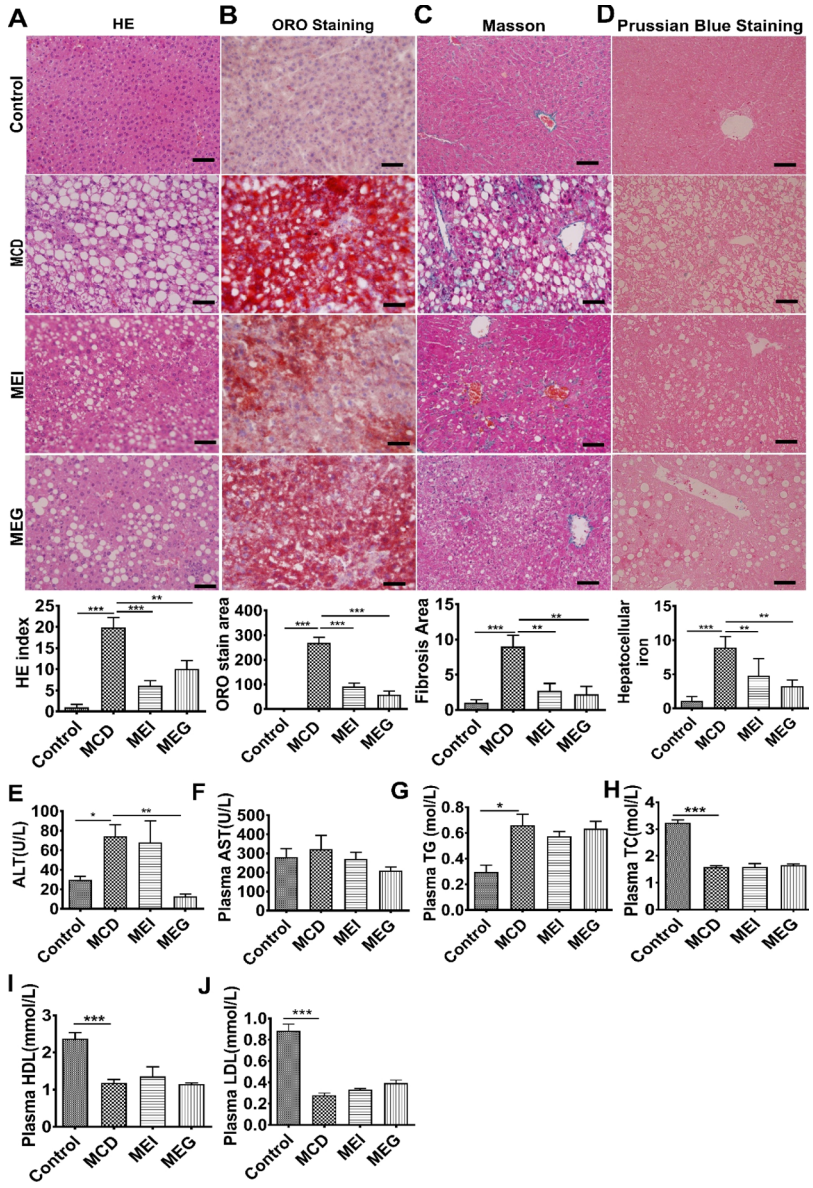

Figure 2. EGCG alleviated hepatic injury, lipid accumulation, fibrosis progression, iron-ion loading, and plasma parameters in MCD-fed mice. (A) Histological sections of the liver from the four groups stained with HE and quantification of the microvesicular steatosis area (at the bottom). (B) Visualization and quantification of neutral lipids by ORO analysis of the frozen liver section (red-droplet). (C) Visualization and quantification of fibrosis severity by Masson's trichrome staining (blue-collagen fibers). (D) Prussian blue staining analysis of iron-ion loading from liver sections (light green-iron ion). (E,F) ALT and AST contents in plasma. (G–J) Relative TG, TC, HDL, and LDL concentrations in plasma. All the above stained results were analyzed and quantified using Image-Pro Plus software and GraphPad Prism Version 6. The values were shown as the mean ± SD values of each group (*P < 0.05, **P < 0.01, ***P < 0.001). n = 4–8. Scare bar: 50 μm.

markedly lower iron accumulation than the MCD group (p < 0.01) (Figure 2D).

It has been demonstrated that plasma parameters were also key indicators to the pathological development of NASH, which were potentially evident in the MCD-induced NASH mouse model in our study. Compared with the control group, the MCD group displayed significantly increased plasma levels of alanine aminotransferase (ALT) (p < 0.05). After 2 weeks of intervention of EGCG, increasing ALT levels were reduced in the MEI and MEG groups (Figure 2E). Moreover, aspartate aminotransferase (AST) has no significant change in the four groups (Figure 2F). Interestingly, the increased triglyceride (TG) levels and the decreased total cholesterol (TC) levels in MCD mice (p < 0.05) have no significant change after supplementation of EGCG (Figure 2G,H), accompanied by the markedly decreased plasma high-density lipoprotein-cholesterol (HDL-C) and low-density lipoprotein-cholesterol (LDL-C) levels in MCD mice (Figure 2I,J).

EGCG Shifting the Microbiome Dysbiosis Induced by the MCD Diet. Next, we determined the gut microbiota composition by 16S ribosomal RNA (rRNA) sequencing. A total of 976,951 raw reads in all samples were generated by high-throughput Illumina sequencing. In addition, 624,087 clean tags were subjected to the subsequent analysis, and validated reads were assembled into operation classification units (OTUs) based on the similarity level at 97%. No significant difference was displayed in the community richness (Ace and Chao) among all groups, while the community diversity (Simpson and Shannon)

https://dx.doi.org/10.1021/acsomega.0c01689
ACS Omega 2020, 5, 20800–20809

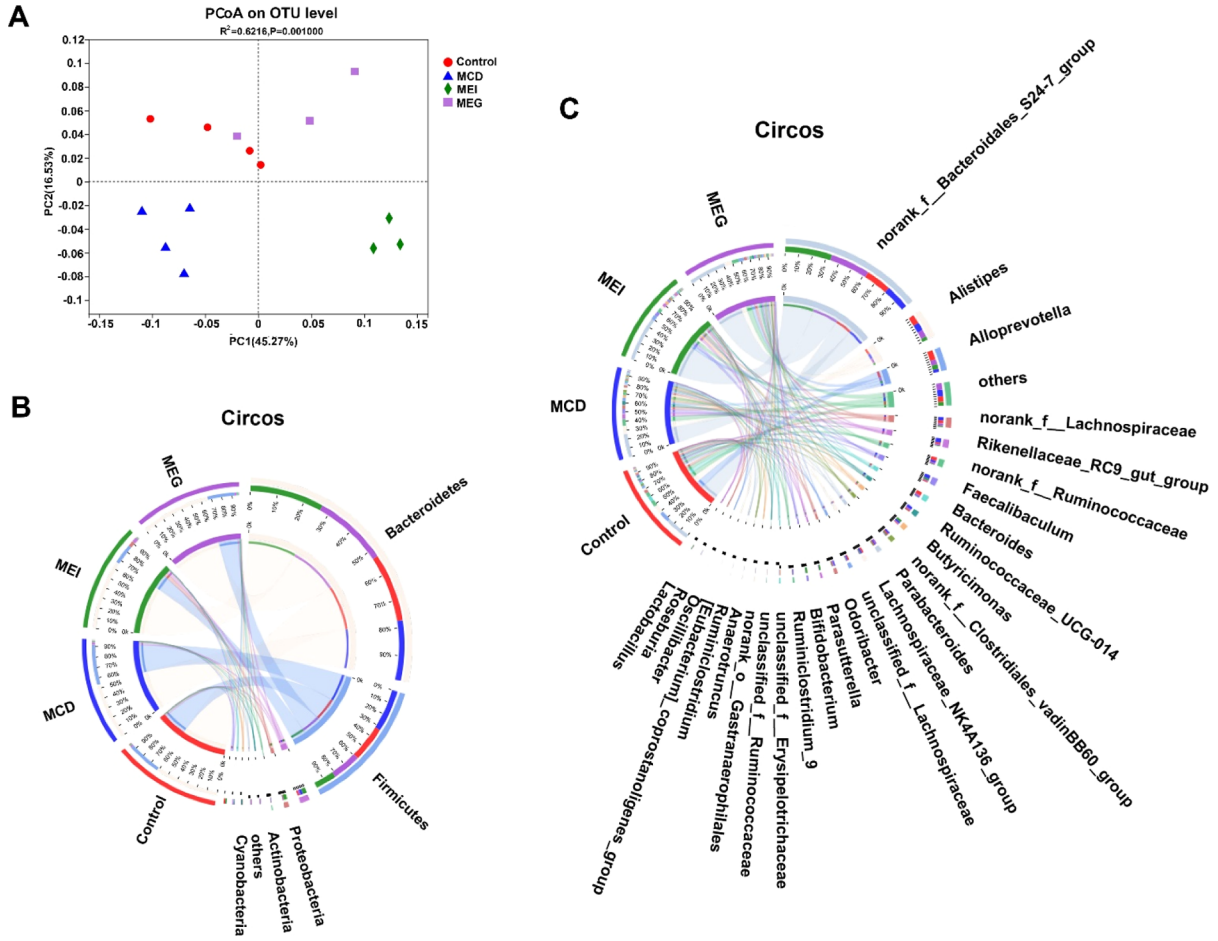

Figure 3. EGCG shifting the microbiome dysbiosis driven by MCD-induced NASH. (A) Beta diversity of MCD-induced microbiota dysbiosis and effects of EGCG analyzed by PCoA. PCoA was performed by using the Bray−Curtis analysis method to calculate the distance between the four groups in faecal samples. The percentages shown on each axis explain the proportion of each dimension. (B,C) Relative abundance of bacterial phyla (B) and genus (C) levels in the control, MCD, MEI, and MEG mice. The percentages on the left half circle represent the ratio of phylum or genus in a certain experimental group. The percentages on the right half circle represent the ratio of different groups in a certain bacteria phylum or genus. The sizes of circles represent the relative abundance of the taxa. n = 3−4.

was significantly decreased after EGCG treatment (Figure S1A−D). Unsupervised multivariate statistical methods such as principal-coordinate analysis (PCoA) were used to assess structural alterations of gut microbiota. As shown in Figure 3A, the MCD group showed an obvious aggregation with the control. The MEI group had developed a new intestinal microbiota balance which was different from neither the MCD group nor the control group.

Analysis at the phylum level showed that the relative abundance of *Bacteroidetes* in the MCD group was notably decreased, while EGCG intervention could partly restore these changes, which enriched EGCG-induced *Bacteroidetes* and decreased the *Firmicutes* ($p < 0.05$) (Figure 3B). In Figure 3C, the relative abundance of *Bacteroides* and *Alloprevotella* belonging to the *Bacteroidetes* phylum was partly decreased in MCD-fed mice. However, the relative abundance of *norank_f__Bacteroidales_S24_7_group*, *Alloprevotella* belonging to *Bacteroidetes,* and *Bifidobacteria* and *Lactobucillus* belonging to *Firmicutes* was increased after EGCG supplementation, especially in the MEI group. *Oxalobacter*, *norank_f__Flavobacteriaceae*, *Oscillibacter*, *Coprococcus_1,* and *Desulfovibrio* were also significantly increased in NASH mice ($p < 0.05$). Importantly, *Alistipes*, *Anaerotruncu*, and *Desulfovibrio*, associated with obesity and the related metabolic disorder, were lower after EGCG administration in NASH mice (Figure 4A, see also Table S1). The results outlined above indicated that EGCG could shift the gut microbiota dysbiosis driven by MCD-induced NASH.

To further illustrate the effects of the altered microbial community, we were subjected to analyze the correlation of altered genus and hepatic injury indexes. Details are as follows: 20 top microbial genera with significantly altered relative abundance between the MCD group and the EGCG-treated group (MEI and MEG), which have a correlation with the representative injury parameters. As shown in the Spearman correlation heatmap, *norank_f__Ruminococcaceae* displayed a significant positive correlation with both TC and TG ($p < 0.05$). *Parasutterella* and *Ruminiclostridium_9* were distinctively positively correlated with the ALT and HE scores ($p < 0.05$), respectively. The fibrosis score was positively correlated with *Bifidobacterium* and negatively correlated with *Alloprevotella* ($p < 0.05$). The neutral lipid area was significantly positively correlated with *Odoribacter*, *Butyricimonas,* and *Ruminiclostridium 9* and negatively correlated with *Bacteroides* and *Alloprevotella* ($p < 0.05$). Unclassified_f__*Ruminococcaceae* was significantly negatively correlated with iron loading ($p < 0.05$) (Figure 4B, see also Figure S2).

https://dx.doi.org/10.1021/acsomega.0c01689
ACS Omega 2020, 5, 20800−20809

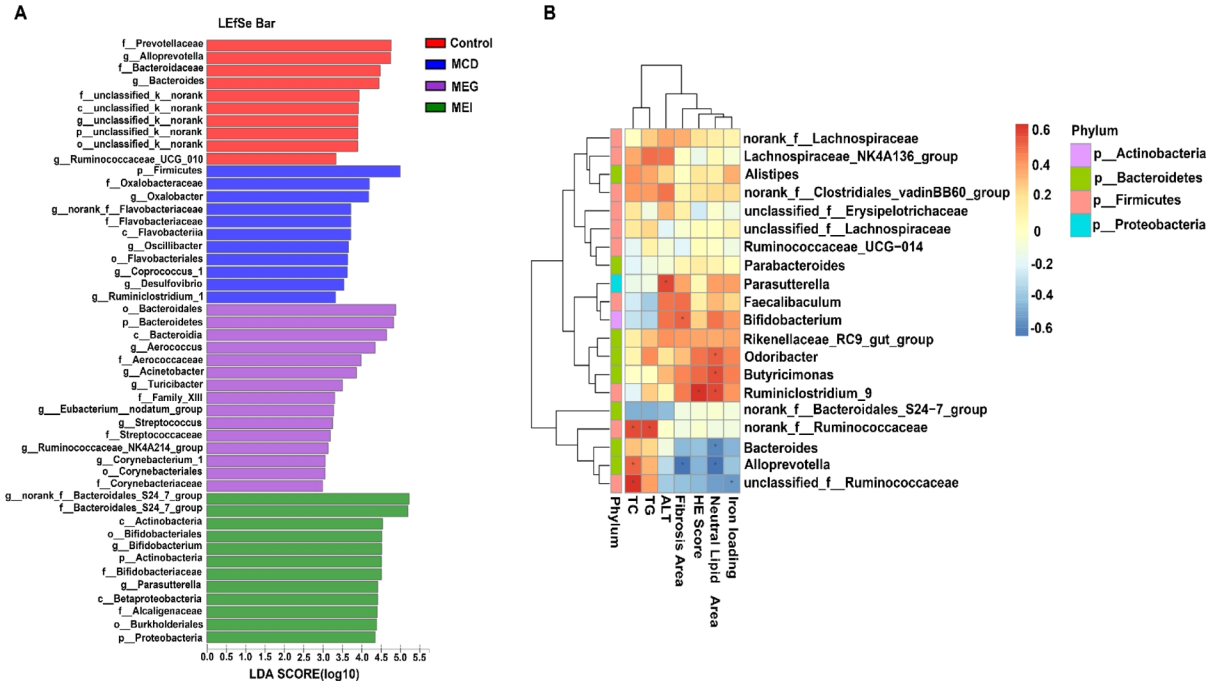

Figure 4. EGCG altered the microbiome dysbiosis driven by MCD-induced NASH interacting with the index of hepatic injury. (A) LEfSe analysis was used to distinguish the differential microbiome between two groups. The criterion for LEfSe was set as LDA > 2 with $p < 0.05$. LDA was representing the taxon enriched in the control (red), MCD (blue), MEI (green), and MEG (purple). The left side represents the name of the bacteria and the classification level to which they belong to. p-phylum, c-class, o-order, f-family, and g-genus. (B) Spearman-correlation heatmap analysis was performed at the representative top 20 microbial genuses and plasma TC, TG, ALT, liver fibrosis area, HE score, neutral droplet area, and iron loading score. There are significant associations with $p < 0.05$ and $r > 0.5$ or $r < 0.5$. $n = 3–4$.

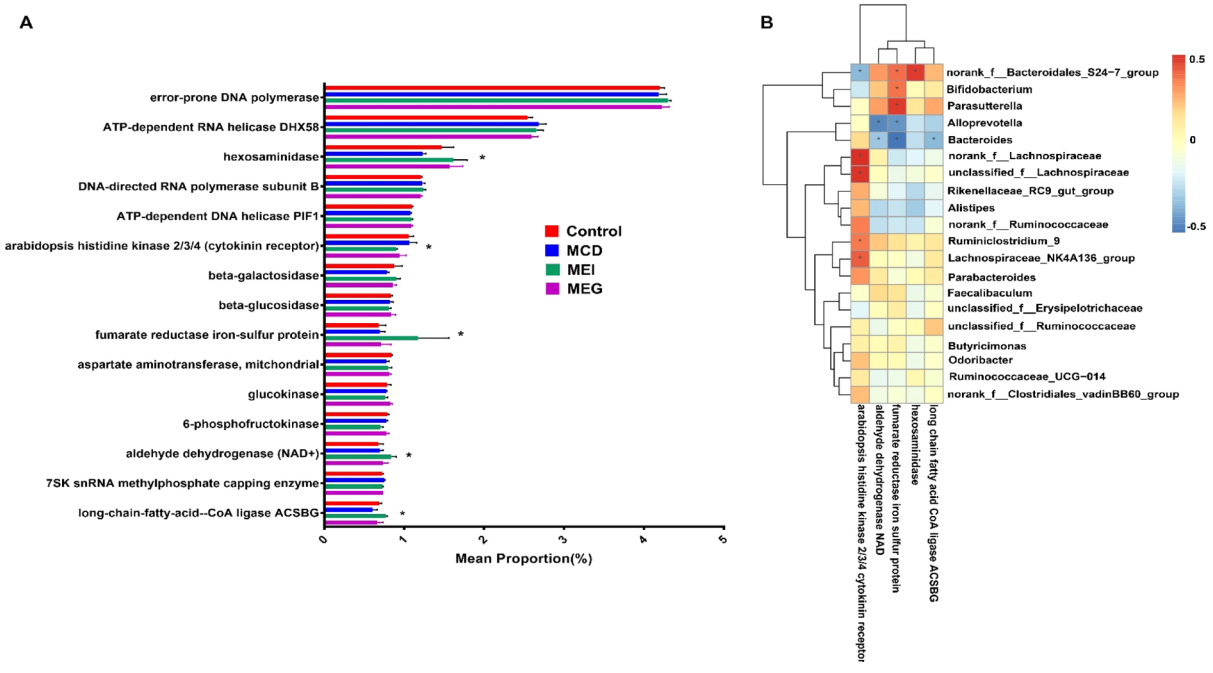

Figure 5. Differential metabolic enzymes predicted by PICRUSt between untreated and EGCG-treated mice. (A) Differential metabolic enzymes predicted by PICRUSt between untreated and the 50 mg/kg EGCG-treated mice. (B) Spearman-correlation heatmap analysis was performed at the representative top 20 microbial genuses and top 50 metabolic enzymes. After variance inflation factor (VIF) screening (VIF < 10), hexosaminidase, arabidopsis_histidine_kinase_2_3_4__cytokinin_receptor, fumarate_reductase_iron_sulfur_protein, aldehyde_dehydrogenase__NAD__, and long-chain-fatty-acid-CoA_ligase_ACSBG were shown. VIF analysis is a commonly used environmental factor screening method, which excludes the interaction between environmental factors themselves. There are significant associations with $P < 0.05$ and $r > 0.5$ or $r < -0.5$. $n = 3–4$.

Predictive Functional Analysis of EGCG Supplementation to MCD-Fed Mice. The functional enzymes and pathways of the gut flora after EGCG treatment were predicted by PICRUSt. There were 1468 enzymes based on OTU predicted by Picrust software (Table S2). In addition, 371 enzymes were changed significantly before and after EGCG treatment (Table

https://dx.doi.org/10.1021/acsomega.0c01689
ACS Omega 2020, 5, 20800−20809

S3). Here, we just showed the top 15 abundant enzymes (Figure 5A). Among these highly abundant enzymes, hexosaminidase is involved in glycan metabolism, arabidopsis histidine kinase 2/3/4 (a cytokinin receptor) belongs to the Quorum sensing pathway, β-galactosidase and glucokinase are related to insulin secretion and sphingolipid metabolism, respectively, and long-chain-fatty-acid-CoA ligase ACSBG plays a critical role in fatty acid metabolism and the ferroptosis pathway (Table S4).

Then, we analyzed the interaction between the representative microbial genera and metabolic enzymes (Figure 5B, see also Figure S3). These enzymes were screened after VIP screening (Table S5). The results indicated that long-chain-fatty-acid-CoA ligase ACSBG had a significant negative correlation with the *Bacteroides* genus ($p < 0.05$); hexosaminidase was significantly positively correlated with *norank_f_Bacteroidales_S24-7_group* ($p < 0.05$); fumarate reductase iron−sulfur protein was significantly positively correlated with *norank_f_Bacteroidales_S24-7_group* and *Bifidobacteria* and *Parasutterlla* ($p < 0.05$); fumarate reductase iron−sulfur protein and aldehyde dehydrogenase (NAD^+) were both significantly negatively correlated with *Alloprevotella* and *Bacteroides* ($p < 0.05$); arabidopsis histidine kinase 2/3/4 (a cytokinin receptor) showed a significant negative correlation with *norank_f_Lachnospiraceae*, unclassified_f_*Lachnospiraceae*, *Ruminiclostridium_9*, and *Lachnospiraceae_NK4A136_group* and a positive correlation with *norank_f_Bacteroidales_S24-7_group* ($p < 0.05$).

DISCUSSION

Emerging evidence suggests the vital role of gut microbiota involved in the development and progression of NAFLD because of microbiota dysbiosis, metabolism disorders, and inflammatory.[41] In addition, several studies have indicated that EGCG, which is an active ingredient from green tea with various biological activities,[25] could exert a beneficial function in NAFLD animal models, but the underlying mechanisms are still undeciphered. Our present data suggest that EGCG showed beneficial effects on MCD-induced NASH, such as serum blood glucose, liver injury, lipid accumulation, iron overload, and microbiota dysbiosis. In addition, oral or i.p. EGCG administration showed a similar therapeutic effect. EGCG could alter the gut microbiota structure and influence the metabolism. Thus, EGCG-moderated NASH mice were described for the new insight through shifting the structure of the gut microbiota and metabolism to alleviate hepatic injury, lipid accumulation, and other pathological features.

Feeding animals with MCD usually causes a body weight loss and metabolism disorders such as NAFLD. Many papers showed that MCD feeding led to a body weight loss while increasing the ratio of liver weight to body weight and finally triggered hepatic steatosis and inflammation. Our data suggested the salutary effect of EGCG on NASH by the reduction in inflammation, macrovesicular fat accumulation, severity of fibrosis, and lowering iron-ion loading as previously reported in the literature.[41,42] Moreover, plasma indexes showed the same trend as histological evaluation. Because of the anatomical position of the liver and gut combining research evidence, "gut−liver axis" was gradually accepted.[43] This proposed theory may help to explain the development of NASH. Gut microbiota dysbiosis leads to bacteria overproliferation and then weakens the intestinal barrier, which may trigger enormous bacteria and products derived from bacteria flow into the blood. Furthermore, bacteria-derived products such as metabolic enzymes could result in altering hepatocyte metabolism, subsequently inducing inflammation and injury, which may involve in NAFLD progression.[44,45] Collectively, EGCG against NAFLD may aim at the gut−liver axis.

In the previous study, EGCG supplementation altered the composition of gut microbiota. Decreasing *Bacteroidetes* and *Firmicutes* enrichment was observed both in humans and in animal models with NAFLD.[45,46] Additionally, regulating intestinal microbiota via added probiotic bacteria can moderate distinctively NAFLD. For example, *Lactobacillus mali* showed beneficial effects on the gut microbiota, characterized by driving growth of *Bacteroidetes*, *Verrucomicrobia*, and *Actinobacteria* while inhibiting *Firmicutes*, lowering serum lipids, and resisting hepatic steatosis.[47−51] Our data revealed that *Bacteroidetes* and *Firmicutes* in MCD mice were enriched and inhibited by EGCG, respectively. Similarly, *Lactobacillus* and *Bifidobacteria*, belonging to the *Firmicutes* phylum that is also related to nutrition and metabolism,[47] were also increased in the EGCG-treated mice. This indicated that EGCG may exert "probiotic-like effects" on NAFLD.[51] Also, other studies suggested that there were some bacteria, such as *Desulfovibrio*, *Alistipes*, and *Anaerotruncu*, which were associated with obesity as well as the related metabolic disorders including NAFLD,[52,53] and interestingly, both of these bacteria genuses were lowered after EGCG was added in NAFLD mice. In addition, *Alloprevotella* belonging to the *Bacteroidetes* phylum has shown anti-inflammatory effects. EGCG addition notably made the *Alloprevotella* genus up in the NASH model. Taken together, EGCG harbored power to lower the body weight via shifting gut microbiota.

To explore whether microbiota dysbiosis influences NASH progression, we further analyzed the correlation between changed genera and ALT, TG, TC, and other pathological features. Correlation analysis is as follows: the representative microbial genera with dramatically changed relative abundance between the MCD group and the EGCG supplementation group (MEI and MEG), which have a correlation with the representative injury parameters. As shown in the Spearman correlation heatmap, *Bacteroides* and *Alloprevotella* belonging to *Bacteroidetes*, which clearly decreased in the MCD group, were significantly negatively correlated with the neutral lipid area. The results suggested that genera of the microbiome structure were involved in the progress of NASH through influencing the pathological features.

Next, functional enzymes of the gut microbiome were predicted by PICRUSt based on OTU. In our study, we found that 1468 enzymes were involved in various metabolic pathways, and 371 enzymes showed distinct changes between the untreated and the EGCG-treated mice. Among these enzymes, long-chain-fatty-acid-CoA ligase ACSBG may play a critical role in fatty acid metabolism and the ferroptosis pathway, suggesting that genera secrete certain enzymes to change metabolism to influence NASH progression. We found that long-chain-fatty-acid-CoA ligase ACSBG has a significant negative correlation with the *Bacteroides* genus. Yao and Craven Seaton et al. identified a group of bacteroides from the intestinal flora, with selective bile brine hydrolysis enzyme activity to help bile acid metabolism.[54] Quan et al. found that myristoleic acid derived from enterococci improved obesity by activating the brown adipose tissue.[55] These studies might have entitled us to aim at certain enzymes to ameliorate the metabolic diseases. Overall, these findings suggested that EGCG can shift gut microbiota and regulate metabolism in MCD-induced NASH mice, thus ameliorating the hepatic injury, lipid accumulation, fibrosis,

https://dx.doi.org/10.1021/acsomega.0c01689
ACS Omega 2020, 5, 20800−20809

and iron loading and thus terminating the inflammatory response. Finally, NASH was prevented.

Although our research tried to provide a valuable insight into the potential influence of EGCG in NASH by regulating gut flora, there still exist several limitations to be addressed in future studies. First, in our results, the microbiota alteration before and after EGCG treatment was just at the genus level and not strain because of the limitations of the sequencing technology we used. Second, although we analyzed the interaction between the representative microbial genera and metabolic enzymes, it was just a prediction and needed further study to confirm that.

CONCLUSIONS

Our findings demonstrated that EGCG exerted protective effects against MCD-diet-induced NASH development. Its work may be through shifting gut microbiota and producing certain enzymes from genera to influence host metabolism. Additionally, oral or i.p. EGCG administration showed similar therapeutic effects. Thus EGCG intervention is a promising strategy for NASH therapy.

MATERIALS AND METHODS

Animals and Treatments. Male C57BL/6J mice (8-week-old) were purchased from Beijing Vital River Laboratory Animal Technology Co., Ltd. After their arrival, the mice were housed in a laminar flow, specific pathogen-free facility and acclimatized for 1 week with free access to a standard chow diet and water in the Laboratory Animal Center, Xi'an Jiaotong University. The animal experiments were approved by the Institutional Animal Ethics Committee of the Xi'an Jiaotong University Health Science Center (no. XJ2018-522). Next, mice were randomly divided into four groups (n = 12/group) and fed with a certain diet for 4 weeks. The control group (control) was given the methionine−choline-sufficient (MCS) diet (Research Diet, New Brunswick, NJ, United States). The MCD group (MCD) was given the MCD diet (Research Diet, New Brunswick, NJ, United States). The MEI group (MEI) was treated with the MCD diet and injected i.p. with EGCG for the last 2 weeks (50 mg/kg, n = 12). The mice of the MEG group (MEG) were given the MCD diet and gavaged with 50 mg/kg of EGCG for the last 2 weeks (50 mg/kg, n = 12). At the end of 4th week, the mice were euthanized by i.p. injection of 4% chloralhydrate (with 1 mg/100 mL atropine) for tissue collection. The body weight was measured once a week, and IPGTT was performed every 2 weeks.

Sample Collection. At the end of week 4, feces samples from all mice were collected and stored at −80 °C for subsequent analysis. Blood samples were collected immediately after anesthesia in mice using ethylenediaminetetraacetic acid-containing tubes and centrifuged at 3000 rpm for 10 min and then kept at −80 °C. Liver tissues were either fixed in 4% neutral-buffered formaldehyde and embedded in paraffin or snap-frozen in liquid nitrogen and stored at −80 °C.

Histological Evaluation of Liver Tissues and Triglycerides and Iron Content. Paraffin-embedded liver sections were stained with hematoxylin−eosin (HE), ORO stain, Masson's trichrome, and Prussian blue to assess liver injury, lipid accumulation, fibrosis, and iron accumulation. The HE score, fibrosis, lipid areas, and iron load were analyzed and quantified using Image-Pro Plus software (version 6.0, Media Cybernetics, Rockville, MD, United States). The macrovesicular (hepatic steatosis) regions, blue regions (collagen), red regions (neutral lipid droplet), and iron overloaded areas were normalized and quantified.

Plasma Parameter Analysis. ALT was measured enzymatically according to the manufacturer's protocol (NanJing JianCheng Bioengineering Institute, China). AST, TG, TC, HDL-C, and LDL-C of plasma were measured using a Beckmann Kurt AU5800 automatic biochemical analyzer.

Microbial Community Analysis in Fecal Samples. DNA extraction from frozen fecal samples (180 mg) was subjected to use an E.Z.N.A Stool DNA kit (Omega, USA) according to the company's protocols. 16S rRNA sequencing was performed using an Illumina MiSeq platform (Illumina, San Diego, U.S.A.). Raw fastq files were quality-filtered by Trimmomatic and FLASH. UPARSE was used to cluster the OTU, with 97% similarity truncation[37,38] (version 7.1 http://drive5.com/uparse/). The community richness (Ace and Chao) and diversity (Shannon and Simpson) were calculated by subsampled data. The taxonomic groups (classes) and genera (subclasses) of bacteria represented by the differences between groups were identified by linear discriminant analysis (LDA) combined with an effector. The LEfSe criterion was set as LDA > 2 with $p < 0.05$.[39] The PICRUSt method was used to infer the metagenomic of intestinal microorganisms from the 16SrRNA sequence.[40] The estimation accuracy of predicting the gene family abundance based on phylogenetic information is 0.8. The predicted functional composition profiles were collapsed into KEGG (Kyoto Encyclopedia of Genes and Genomes) database pathways. Pathways present in <10% of the samples were not involved in the following comparison analysis.

Statistical Analysis. Statistical analysis of the results of the four groups was performed using one-way ANOVA, and Tukey's post hoc test was used to determine the significance.

Data analysis was performed using GraphPad Prism Version 6. Analysis of the sequencing data was carried out using the R software package (V.3.2.1) and the free online Majorbio-Sanger cloud platform (www.i-sanger.com).Spearman's correlation was performed for the correlation heatmap. The Mann−Whitney U test was used for continuous variables, and the Wilcoxon rank sum test was used for non-normal distribution data.

ASSOCIATED CONTENT

Supporting Information

The Supporting Information is available free of charge at https://pubs.acs.org/doi/10.1021/acsomega.0c01689.

Community richness (Ace and Chao) and diversity (Shannon and Simpson) of all sequencing samples; correlation between representative 50 microbial genera and index of hepatic injury; and correlation between representative 50 microbial genera and top 15 metabolic enzymes (PDF)

EGCG shifting microbiota dysbiosis driven by MCD-induced NASH in four groups; functional enzymes of the gut microbiome after EGCG treatment; 371 enzymes showed distinct changes between untreated and the 50 mg/kg EGCG-treated mice; metabolic pathways in which the functional enzymes are located; and VIP screening for the metabolic enzyme (XLSX)

AUTHOR INFORMATION

Corresponding Author

Dongmin Li − *Department of Biochemistry and Molecular Biology, School of Basic Medical Sciences, Xi'an Jiaotong*

https://dx.doi.org/10.1021/acsomega.0c01689
ACS Omega 2020, 5, 20800−20809

University Health Science Center, Xi'an, Shaanxi 710061, P. R. China; Key Laboratory of Environment and Genes Related to Diseases (Xi'an Jiaotong University), Ministry of Education of China, Xi'an, Shaanxi 710061, P. R. China; orcid.org/0000-0002-7808-1109; Email: lidongm@mail.xjtu.edu.cn

Authors

Kaiting Ning − *Department of Biochemistry and Molecular Biology, School of Basic Medical Sciences, Xi'an Jiaotong University Health Science Center, Xi'an, Shaanxi 710061, P. R. China; Key Laboratory of Environment and Genes Related to Diseases (Xi'an Jiaotong University), Ministry of Education of China, Xi'an, Shaanxi 710061, P. R. China*

Kaikai Lu − *Department of Biochemistry and Molecular Biology, School of Basic Medical Sciences, Xi'an Jiaotong University Health Science Center, Xi'an, Shaanxi 710061, P. R. China; Key Laboratory of Environment and Genes Related to Diseases (Xi'an Jiaotong University), Ministry of Education of China, Xi'an, Shaanxi 710061, P. R. China*

Qian Chen − *Department of Biochemistry and Molecular Biology, School of Basic Medical Sciences, Xi'an Jiaotong University Health Science Center, Xi'an, Shaanxi 710061, P. R. China; Key Laboratory of Environment and Genes Related to Diseases (Xi'an Jiaotong University), Ministry of Education of China, Xi'an, Shaanxi 710061, P. R. China*

Zizhen Guo − *Shanghai Jiao Tong University School of Medicine, Shanghai 200025, P. R. China*

Xiaojuan Du − *Department of Biochemistry and Molecular Biology, School of Basic Medical Sciences, Xi'an Jiaotong University Health Science Center, Xi'an, Shaanxi 710061, P. R. China; Key Laboratory of Environment and Genes Related to Diseases (Xi'an Jiaotong University), Ministry of Education of China, Xi'an, Shaanxi 710061, P. R. China*

Farooq Riaz − *Department of Biochemistry and Molecular Biology, School of Basic Medical Sciences, Xi'an Jiaotong University Health Science Center, Xi'an, Shaanxi 710061, P. R. China; Key Laboratory of Environment and Genes Related to Diseases (Xi'an Jiaotong University), Ministry of Education of China, Xi'an, Shaanxi 710061, P. R. China*

Lina Feng − *Department of Biochemistry and Molecular Biology, School of Basic Medical Sciences, Xi'an Jiaotong University Health Science Center, Xi'an, Shaanxi 710061, P. R. China; Key Laboratory of Environment and Genes Related to Diseases (Xi'an Jiaotong University), Ministry of Education of China, Xi'an, Shaanxi 710061, P. R. China*

Yuping Fu − *Department of Cardiology, The Second Affiliated Hospital, Xi'an Jiaotong University, Xi'an 710004, China*

Chunyan Yin − *Department of Pediatric, The Second Affiliated Hospital, Xi'an Jiaotong University, Xi'an 710004, China*

Fujun Zhang − *Department of Biochemistry and Molecular Biology, School of Basic Medical Sciences, Xi'an Jiaotong University Health Science Center, Xi'an, Shaanxi 710061, P. R. China; Key Laboratory of Environment and Genes Related to Diseases (Xi'an Jiaotong University), Ministry of Education of China, Xi'an, Shaanxi 710061, P. R. China*

Litao Wu − *Department of Biochemistry and Molecular Biology, School of Basic Medical Sciences, Xi'an Jiaotong University Health Science Center, Xi'an, Shaanxi 710061, P. R. China; Key Laboratory of Environment and Genes Related to Diseases (Xi'an Jiaotong University), Ministry of Education of China, Xi'an, Shaanxi 710061, P. R. China*

Complete contact information is available at: https://pubs.acs.org/10.1021/acsomega.0c01689

Author Contributions

K.N. and K.L. contributed equally to this study. K.N., K.L., C.Y., and D.L. contributed to the study design; K.N., K.L., Q.C., X.D., L.F., Y.F., F.Z., and L.W. performed the experiments; K.N., K.L., Z.G.,and F.R. participated in writing and revising this article. K.N. drew the TOC picture. All authors participated in the final approval of this article.

Notes

The authors declare no competing financial interest.

■ ACKNOWLEDGMENTS

This work was supported by the National Natural Science Foundation of China (grant numbers 81770864 and 81370952) and the Fundamental Research Funds for the Central Universities (grant number zrzd2017007). We thank Prof. Jiru Xu and Dr. Huan Li of the Laboratory of Microbiology and Immunology, Xi'an Jiaotong University School of Medicine, for supporting our experiments. We thank Xin Liu of Shanghai Major Biotechnology Co., Ltd. for his professional service.

■ ABBREVIATIONS

EGCG, epigallocatechin gallate; NASH, nonalcoholic steatohepatitis; NAFLD, nonalcoholic fatty liver disease; NAFL, nonalcoholic fatty liver; MCS (control diet), methionine−choline-sufficient diet; MCD, methionine−choline-deficient diet; LPS, lipopolysaccharide; SCFAs, short-chain fatty acids; IPGTT, intraperitoneal glucose tolerance test; MEI, MCD diet + intraperitoneal EGCG (50 mg/kg); MEG, MCD diet + gavage EGCG (50 mg/kg); ORO, Oil red O stain; Masson, Masson's trichrome; HE, hematoxylin−eosin; ALT, alanine aminotransferase; AST, aspartate aminotransferase; TC, total cholesterol; TG, triglyceride; HDL-C (HDL), high-density lipoprotein-cholesterol; LDL-C (LDL), low-density lipoprotein-cholesterol; OTUs, operational taxonomic units; PCoA, principal coordinate analysis; NMDS, nonmetric multidimensional scaling; LEfSe, linear discriminant analysis (LDA) effect size; ANOVA, analysis of variance

■ REFERENCES

(1) Brunt, E. M.; Wong, V. W.-S.; Nobili, V.; Day, C. P.; Sookoian, S.; Maher, J. J.; Bugianesi, E.; Sirlin, C. B.; Neuschwander-Tetri, B. A.; Rinella, M. E. Nonalcoholic fatty liver disease. *Nat. Rev. Dis. Primers* **2015**, *1*, 15080.

(2) Cai, J.; Zhang, X.-J.; Li, H. Role of Innate Immune Signaling in Non-Alcoholic Fatty Liver Disease. *Trends Endocrinol. Metab.* **2018**, *29*, 712−722.

(3) Loomba, R.; Sirlin, C. B.; Ang, B.; Bettencourt, R.; Jain, R.; Salotti, J.; Soaft, L.; Hooker, J.; Kono, Y.; Bhatt, A.; et al. Ezetimibe for the treatment of nonalcoholic steatohepatitis: assessment by novel magnetic resonance imaging and magnetic resonance elastography in a Randomized trial (MOZART trial). *Hepatology* **2015**, *61*, 1239−1250.

(4) Woodhouse, C. A.; Patel, V. C.; Singanayagam, A.; Shawcross, D. L. Review article: the gut microbiome as a therapeutic target in the pathogenesis and treatment of chronic liver disease. *Aliment. Pharmacol. Ther.* **2018**, *47*, 192−202.

(5) Brandl, K.; Schnabl, B. Intestinal microbiota and nonalcoholic steatohepatitis. *Curr. Opin. Gastroenterol.* **2017**, *33*, 128−133.

(6) Aqel, B.; DiBaise, J. K. Role of the gut microbiome in nonalcoholic fatty liver disease. *Nutr. Clin. Pract.* **2015**, *30*, 780−786.

(7) Moschen, A. R.; Kaser, S.; Tilg, H. Non-alcoholic steatohepatitis: a microbiota-driven disease. *Trends Endocrinol. Metab.* **2013**, *24*, 537−545.

(8) Adolph, T. E.; Grander, C.; Tilg, A. R.; Herbert, T. liver-Microbiome axis in Health and Disease. *Trends Immunol.* **2018**, *39*, 712−723.
(9) Paolella, G.; Mandato, C.; Pierri, L.; Poeta, M.; Di Stasi, M.; Vajro, P. Gut-liver axis and probiotics: their role in non-alcoholic fatty liver disease. *World J. Gastroenterol.* **2014**, *20*, 15518−15531.
(10) Miele, L.; Marrone, G.; Lauritano, C.; Cefalo, C.; Gasbarrini, A.; Day, C.; Grieco, A. Gut-liver axis and microbiota in NAFLD: insight pathophysiology for novel therapeutic target. *Curr. Pharm. Des.* **2013**, *19*, 5314−5324.
(11) Littman, D. R.; Pamer, E. G. Role of the commensal microbiota in normal and pathogenic host immune responses. *Cell Host Microbe* **2011**, *10*, 311−323.
(12) Henao-Mejia, J.; Elinav, E.; Jin, C.; Hao, L.; Mehal, W. Z.; Strowig, T.; Thaiss, C. A.; Kau, A. L.; Eisenbarth, S. C.; Jurczak, M. J.; et al. Inflammasome-mediated dysbiosis regulates progression of NAFLD and obesity. *Nature* **2012**, *482*, 179−185.
(13) Allaire, J. M.; Crowley, S. M.; Law, H. T.; Chang, S.-Y.; Ko, H.-J.; Vallance, B. A. The Intestinal Epithelium: Central Coordinator of Mucosal Immunity. *Trends Immunol.* **2019**, *40*, 174.
(14) Peng, L.; Li, Z.-R.; Green, R. S.; Holzman, I. R.; Lin, J. Butyrate enhances the intestinal barrier by facilitating tight junction assembly via activation of AMP-activated protein kinase in Caco-2 cell monolayers. *J. Nutr.* **2009**, *139*, 1619−1625.
(15) Farrell, G. C.; van Rooyen, D. Liver cholesterol: is it playing possum in NASH? *Am. J. Physiol.: Gastrointest. Liver Physiol.* **2012**, *303*, G9−G11.
(16) Puri, P.; Wiest, M. M.; Cheung, O.; Mirshahi, F.; Sargeant, C.; Min, H.-K.; Contos, M. J.; Sterling, R. K.; Fuchs, M.; Zhou, H.; et al. The plasma lipidomic signature of nonalcoholic steatohepatitis. *Hepatology* **2009**, *50*, 1827−1838.
(17) Fujita, N.; Miyachi, H.; Tanaka, H.; Takeo, M.; Nakagawa, N.; Kobayashi, Y.; Iwasa, M.; Watanabe, S.; Takei, Y. Iron overload is associated with hepatic oxidative damage to DNA in nonalcoholic steatohepatitis. *Cancer Epidemiol., Biomarkers Prev.* **2009**, *18*, 424−432.
(18) Philippe, M. A.; Ruddell, R. G.; Ramm, G. A. Role of iron in hepatic fibrosis: one piece in the puzzle. *World J. Gastroenterol.* **2007**, *13*, 4746−4754.
(19) Seki, S.; Kitada, T.; Yamada, T.; Sakaguchi, H.; Nakatani, K.; Wakasa, K. In situ detection of lipid peroxidation and oxidative DNA damage in non-alcoholic fatty liver diseases. *J. Hepatol.* **2002**, *37*, 56−62.
(20) Chen, W. J.; Cai, B.; Chen, H. T.; Cao, C. Y.; Du, Y. L.; Li, Y. Y.; Nie, Y. Q.; Zhou, Y. J. The Role of ADIPOQ Methylation in Experimental Non-alcoholic Fatty Liver Disease: ADIPOQ Methylation in NAFLD. *J. Dig. Dis.* **2016**, *17*, 829−836.
(21) Ohshima, S.; Horie, Y.; Kinoshita, N.; Ishii, H.; Anezaki, Y.; Miura, K.; Goto, T.; Suzuki, A.; Ohnishi, H. S1837 UDCA Improves Liver Inflammation of NASH by Reducing ROS Levels and Increasing the Expression of NRF2-Regulated Antioxident Genes-an Examination Using Hepatocyte-Specific PTEN Deficient Mice. *Gastroenterology* **2010**, *138*, S799−S800.
(22) Wolf, A.; Bray, G. A.; Popkin, B. M. A short history of beverages and how our body treats them. *Obes. Rev.* **2008**, *9*, 151−164.
(23) Cabrera, C.; Artacho, R.; Giménez, R. Beneficial effects of green tea–a review. *J. Am. Coll. Nutr.* **2006**, *25*, 79−99.
(24) Khan, N.; Mukhtar, H. Tea polyphenols for health promotion. *Life Sci.* **2007**, *81*, 519−533.
(25) Chen, D.; Milacic, V.; Chen, M. S.; Wan, S. B.; Lam, W. H.; Huo, C.; Landis-Piwowar, K. R.; Cui, Q. C.; Wali, A.; Chan, T. H.; et al. Tea polyphenols, their biological effects and potential molecular targets. *Histol. Histopathol.* **2008**, *23*, 487−496.
(26) Thielecke, F.; Boschmann, M. The potential role of green tea catechins in the prevention of the metabolic syndrome - a review. *Phytochemistry* **2009**, *70*, 11−24.
(27) Klaus, S.; Pültz, S.; Thöne-Reineke, C.; Wolfram, S. Epigallocatechin gallate attenuates diet-induced obesity in mice by decreasing energy absorption and increasing fat oxidation. *Int. J. Obes.* **2005**, *29*, 615−623.
(28) Wolfram, S. Effects of green tea and EGCG on cardiovascular and metabolic health. *J. Am. Coll. Nutr.* **2007**, *26*, 373S−388S.
(29) Bose, M.; Lambert, J. D.; Ju, J.; Reuhl, K. R.; Shapses, S. A.; Yang, C. S. The major green tea polyphenol, (-)-epigallocatechin-3-gallate, inhibits obesity, metabolic syndrome, and fatty liver disease in high-fat-fed mice. *J. Nutr.* **2008**, *138*, 1677−1683.
(30) Friedrich, M.; Petzke, K. J.; Raederstorff, D.; Wolfram, S.; Klaus, S. Acute effects of epigallocatechin gallate from green tea on oxidation and tissue incorporation of dietary lipids in mice fed a high-fat diet. *Int. J. Obes.* **2012**, *36*, 735.
(31) Gan, L.; Meng, Z.-j.; Xiong, R.-b.; Guo, J.-q.; Lu, X.-c.; Zheng, Z.-w.; Deng, Y.-p.; Luo, B.-d.; Zou, F.; Li, H. Green tea polyphenol epigallocatechin-3-gallate ameliorates insulin resistance in non-alcoholic fatty liver disease mice. *Acta Pharmacol. Sin.* **2015**, *36*, 597−605.
(32) Ding, Y.; Sun, X.; Chen, Y.; Deng, Y.; Qian, K. Epigallocatechin gallate attenuated non-alcoholic steatohepatitis induced by methionine- and choline-deficient diet. *Eur. J. Pharmacol.* **2015**, *761*, 405−412.
(33) Yu, J.; Marsh, S.; Hu, J.; Feng, W.; Wu, C. Gut Microbiota and Metagenomic Advancement in Digestive Disease. *Gastroent. Res. Pract.* **2016**, *2016*, 4703406.
(34) Marchesini, G.; Mazzotti, A. NAFLD incidence and remission: only a matter of weight gain and weight loss? *J. Hepatol.* **2015**, *62*, 15−17.
(35) Kochi, T.; Shimizu, M.; Terakura, D.; Baba, A.; Ohno, T.; Kubota, M.; Shirakami, Y.; Tsurumi, H.; Tanaka, T.; Moriwaki, H. Non-alcoholic steatohepatitis and preneoplastic lesions develop in the liver of obese and hypertensive rats: suppressing effects of EGCG on the development of liver lesions. *Cancer Lett.* **2014**, *342*, 60−69.
(36) Viollet, B.; Guigas, B.; Leclerc, J.; Hébrard, S.; Lantier, L.; Mounier, R.; Andreelli, F.; Foretz, M. AMP-activated protein kinase in the regulation of hepatic energy metabolism: from physiology to therapeutic perspectives. *Acta Physiol.* **2009**, *196*, 81−98.
(37) Caporaso, J. G.; Kuczynski, J.; Stombaugh, J.; Bittinger, K.; Bushman, F. D.; Costello, E. K.; Fierer, N.; Peña, A. G.; Goodrich, J. K.; Gordon, J. I.; et al. QIIME allows analysis of high-throughput community sequencing data. *Nat. Methods* **2010**, *7*, 335−336.
(38) Cole, J. R.; Wang, Q.; Cardenas, E.; Fish, J.; Chai, B.; Farris, R. J.; Kulam-Syed-Mohideen, A. S.; McGarrell, D. M.; Marsh, T.; Garrity, G. M.; et al. The ribosomal database project: improved alignments and new tools for rRNA analysis. *Nucleic Acids Res.* **2009**, *37*, D141−D145.
(39) Lu, H.; Ren, Z.; Li, A.; Zhang, H.; Jiang, J.; Xu, S.; Luo, Q.; Zhou, K.; Sun, X.; Zheng, S.; et al. Deep sequencing reveals microbiota dysbiosis of tongue coat in patients with liver carcinoma. *Sci. Rep.* **2016**, *6*, 33142.
(40) Langille, M. G. I.; Zaneveld, J.; Caporaso, J. G.; McDonald, D.; Knights, D.; Reyes, J. A.; Clemente, J. C.; Burkepile, D. E.; Vega Thurber, R. L.; Knight, R.; et al. Predictive functional profiling of microbial communities using 16S rRNA marker gene sequences. *Nat. Biotechnol.* **2013**, *31*, 814−821.
(41) Ye, J.; Lv, L.; Wu, W.; Li, Y.; Ding, S.; Fang, D.; Guo, F.; Jiang, H.; Ren, Y.; Ye, W.; et al. Butyrate Protects Mice Against Methionine−Choline-Deficient Diet-Induced Non-alcoholic Steatohepatitis by Improving Gut Barrier Function, Attenuating Inflammation and Reducing Endotoxin Levels. *Front. Microbiol.* **2018**, *9*, 1967.
(42) Simon, Y.; Kessler, S. M.; Gemperlein, K.; Bohle, R. M.; Müller, R.; Haybaeck, J.; Kiemer, A. K. Elevated free cholesterol in a p62 overexpression model of non-alcoholic steatohepatitis. *World J. Gastroenterol.* **2014**, *20*, 17839−17850.
(43) Tripathi, A.; Debelius, J.; Brenner, D. A.; Karin, M.; Loomba, R.; Schnabl, B.; Knight, R. The gut−liver axis and the intersection with the microbiome. *Nat. Rev. Gastroenterol. Hepatol.* **2018**, *15*, 397.
(44) Caussy, C.; Loomba, R. Gut microbiome, microbial metabolites and the development of NAFLD. *Nat. Rev. Gastroenterol. Hepatol.* **2018**, *15*, 719−720.
(45) Jiang, W.; Wu, N.; Wang, X.; Chi, Y.; Zhang, Y.; Qiu, X.; Hu, Y.; Jing, L.; Liu, Y. Dysbiosis gut microbiota associated with inflammation and impaired mucosal immune function in intestine of humans with non-alcoholic fatty liver disease. *Sci. Rep.* **2015**, *5*, 8096.

https://dx.doi.org/10.1021/acsomega.0c01689
ACS Omega 2020, 5, 20800−20809

(46) Lin, P.; Lu, J.; Wang, Y.; Gu, W.; Yu, J.; Zhao, R. Naturally Occurring Stilbenoid TSG Reverses Non-Alcoholic Fatty Liver Diseases via Gut-Liver Axis. *PLoS One* **2015**, *10*, No. e0140346.
(47) Ritze, Y.; Bárdos, G.; Claus, A.; Ehrmann, V.; Bergheim, I.; Schwiertz, A.; Bischoff, S. C. Lactobacillus rhamnosus GG protects against non-alcoholic fatty liver disease in mice. *PLoS One* **2014**, *9*, No. e80169.
(48) Chen, Y.-T.; Yang, N.-S.; Lin, Y.-C.; Ho, S.-T.; Li, K.-Y.; Lin, J.-S.; Liu, J.-R.; Chen, M.-J. Combination of Lactobacillus mali APS1 and dieting improved the efficacy of obesity treatment via manipulating gut microbiome in mice. *Sci. Rep.* **2018**, *8*, 6153.
(49) Everard, A.; Matamoros, S.; Geurts, L.; Delzenne, N. M.; Cani, P. D. Saccharomyces boulardii administration changes gut microbiota and reduces hepatic steatosis, low-grade inflammation, and fat mass in obese and type 2 diabetic db/db mice. *mBio* **2014**, *5*, No. e01011-14.
(50) Neyrinck, A. M.; Possemiers, S.; Druart, C.; Van de Wiele, T.; De Backer, F.; Cani, P. D.; Larondelle, Y.; Delzenne, N. M. Prebiotic effects of wheat arabinoxylan related to the increase in bifidobacteria, Roseburia and Bacteroides/Prevotella in diet-induced obese mice. *PLoS One* **2011**, *6*, No. e20944.
(51) Lambert, J. E.; Parnell, J. A.; Eksteen, B.; Raman, M.; Bomhof, M. R.; Rioux, K. P.; Madsen, K. L.; Reimer, R. A. Gut microbiota manipulation with prebiotics in patients with non-alcoholic fatty liver disease: a randomized controlled trial protocol. *BMC Gastroenterol.* **2015**, *15*, 169.
(52) Shin, N.-R.; Lee, J.-C.; Lee, H.-Y.; Kim, M.-S.; Whon, T. W.; Lee, M.-S.; Bae, J.-W. An increase in the Akkermansia spp. population induced by metformin treatment improves glucose homeostasis in diet-induced obese mice. *Gut* **2014**, *63*, 727−735.
(53) Zhang, C.; Zhang, M.; Pang, X.; Zhao, Y.; Wang, L.; Zhao, L. Structural resilience of the gut microbiota in adult mice under high-fat dietary perturbations. *ISME J.* **2012**, *6*, 1848−1857.
(54) Yao, L.; Craven Seaton, S.; Ndousse-Fetter, S.; Adhikari, A. A.; Di Benedetto, N.; Mina, A. I.; et al. A selective gut bacterial bile salt hydrolase alters host metabolism. *Elife* **2018**, *7*, No. e37182.
(55) Quan, L.-H.; Zhang, C.; Dong, M.; Jiang, J.; Xu, H.; Yan, C.; Liu, X.; Zhou, H.; Zhang, H.; Chen, L.; et al. Myristoleic acid produced by enterococci reduces obesity through brown adipose tissue activation. *Gut* **2020**, *69*, 1239.

https://dx.doi.org/10.1021/acsomega.0c01689
ACS Omega 2020, 5, 20800−20809